Results in Chemistry 18 (2025) 102742

Contents lists available at ScienceDirect

Results in Chemistry

journal homepage: www.sciencedirect.com/journal/results-in-chemistry

Molecular hybrid design, physicochemical, and thermal properties of new five quinoline sulfonyl hydrazide Schiff base derivatives: bioinformatics and antibacterial investigation

H. Qrareya [a], S. Sadi [a], L. Abdallah [b], A. Zarrouk [c], F. Al battah [d], I. Warad [e,*]

[a] Department of Applied Chemistry, Arab American University (AAUP), Jenin, P.O Box 240, Palestine
[b] Department of Biology and Biotechnology, Science College, An-Najah National University, Nablus, P.O. Box 7, Palestine
[c] Laboratory of Molecular Spectroscopy Modelling, Materials, Nanomaterials, Water and Environment, CERNE2D, Faculty of Science, Mohammed V University in Rabat, Morocco
[d] Department of Biology and biotechnology, Arab American University (AAUP), Jenin, P.O Box 240, Palestine
[e] Department of Chemistry, Science College, An-Najah National University, Nablus, P.O. Box 7, Palestine

ARTICLE INFO

Keywords:
Quinoline-sulfonohydrazide
NMR
QSHSB
Schiff bases
Docking
Antimicrobial

ABSTRACT

Quinoline-sulfonohydrazide Schiff bases (QSHSB) have been synthesized in a substantial amount through the reflux dehydration of quinoline-8-sulfonohydrazide with various functionalized aldehydes in absolute ethanol and 68–94 % yields. The condensation synthetic reaction of the new QSHSB was tracked via two primary spectroscopic tools such as UV–visible and FT-IR. The optical characteristics of the target QSHSB ligands Tauc's $\Delta E_g = 2.75–4.21$ eV were revealed by effectively coordinating the UV–visible spectra with the experimental Tuac energy gap. Moreover, all the desired QSHSB ligands compositions were subjected additionally to MS, (^{1}H &^{13}C) NMR, CHN-EA, and EDX analysis. According to the TG/DTG results, the ligands are a material with a stable one-step thermal breakdown up to 225 °C. Meanwhile, all QSHSB met the Lipinski's (Ro5) requirements, and the ideal molecular hybrid drug design was determined by docking bioinformatics study with −8.0-11.0 kcal/mol binding energies; the best design included QSHSB **2**, as 4H-bonds with 1BNA were recorded. Moreover, the antimicrobial properties of QSHSB ligands have been demonstrated against both gram-positive and negative bacteria via MIC (62.5–125 μg/mL for **3**), IZD (10–13 mm), and MBC (62.5–500 μg/mL) methods.

1. Introduction

Schiff bases considered to be one of the most important ligands which prepared by condensation of 1° amine with ketones or aldehydes [1–5]. As soft basic catalysts, trimethylamine or pyridine can facilitate this coupling; as acidic catalysts, acetic, sulfuric, or hydrochloric acids can be employed [5]. In comparison to their aliphatic counterparts, aromatic Schiff base ligands are more common because of the enhanced stability that comes from having an aromatic conjugated structure [6].

In general, Schiff base ligands possess numerous applications in several domains of biology, chemistry, and medicine [6–11]. Various biological applications, such as anti-inflammatory, antifungal, antibacterial, anticancer, antioxidant, anti-plasmodia, anti-corrosion and antidepressant were documented [6–11]. Moreover, Schiff base considered as one of the most comprehensive and excellent polychelates or mono-chelates N-ligands in coordinating TM ion centers [10]. Hydrazones Schiff base (HSB) is a distinct category of bases that possess the azomethine functional group, HSB compounds exhibit a broader spectrum of therapeutic effects, encompassing antiepileptic, anti-inflammatory antiviral, antibacterial, antioxidant, analgesic, anti-cancer and anticholinesterase characteristics [6–8]. Sulfonohydrazones Schiff bases (SHSB) mostly have been produced and employed as ligand complexes since of their remarkable chelating capabilities [9–18]. SHSB are commonly acknowledged as antibacterial agents. SHSB and sulfonamides demonstrate antibacterial activity against *S. aureus* and *E. coli* [12,13]. SHSB are believed to work by inhibiting the formation of folic acid, which is important for the survival of bacteria [14]. The synthesis of SHSB has attracted considerable attention since sulfones are important components in pharmaceutical and natural products [15,16]. SHSB have unique chemical properties and are utilized as essential intermediates in synthesis of organic compounds [16–19]. SHSB biological activities, specifically their ability to combat fungal and microbial

* Corresponding author.
E-mail address: warad@najah.edu (I. Warad).

https://doi.org/10.1016/j.rechem.2025.102742
Received 29 June 2025; Accepted 23 September 2025
Available online 24 September 2025

infections, have attracted considerable attention, especially those that involve complexes of transition metal ions with heterocyclic components [19]. The desired result is the attachment of SHSB ligands to the TM center ions, which results in improving antibacterial and antifungal properties compared to the ligands, still a topic that many researchers, including our research group, are competing over to this day.

The design of this new class of quinoline sulfonyl hydrazide Schiff bases has distinct bioinformatics and molecular hybrid problems, especially in reconciling steric restrictions, electronic effects, and pharmacophore compatibility [18]. Quinoline scaffolds have extensive bioactivity, whilst sulfonyl hydrazide Schiff bases provide adaptable coordination and H-bonding properties. Principal problems encompass improving the structural flexibility of the hydrazone linker for target affinity, preserving metabolic stability, and augmenting selectivity against off-target interactions. Moreover, the electronic modification of the quinoline ring and sulfonyl group may affect π-stacking and charge distribution, which are essential for interactions with enzymes, proteins, or DNA. Its purpose is to understand the nature of the bond, explain specific medical outcomes, or predict the potential therapeutic effects of new compounds [20–23].

As our ongoing efforts to synthesis new N-polychelate ligands and their TM complexes [24–27], in this work, five novel QSHSB ligands were synthesized and subjected to characterization utilizing a range of analytical techniques including NMR, FT-IR, MS, EDX, UV–vis, CHN-EA, and TGA analysis, the TG/DTG reflected all prepared Schiff base ligands as thermal stable compounds. The Lipinski's (Ro5) rule of five, together with the 1BNA docking bioinformatics stimulation studies were conducted for all the ligands of interest. Moreover, the antibacterial activities have been proven effective against a wide range of bacteria.

2. Experimental

2.1. Chemicals, instruments and docking

All chemicals and solvents were used as purchased without any purification or distillation. FT-IR spectra were measured in the 400–4000 cm^{-1} range on a (Shimadzu) spectrophotometer. Electronic absorption spectra and Kinetic measurements were obtained using UV-1900I spectrophotometer (Shimadzu). The NMR ($^{1}H\&^{13}C$) spectra were recorded in $CDCl_3$ solution on 400 MHz Jeol GSX WB spectrometer using TMS as an internal reference. The DNA docking simulation was performed using AutoDock Tools v4 [28]. The 3D structural data of duplex DNA (PDB ID: 1BNA) were received from the Protein Data Bank [29]. Before docking simulations, all co-crystal ligands, ions, and water molecules were removed from the proteins. Additionally, charge neutralization, polar hydrogen configurations, and all rotatable bonds were managed by ADT4. Additionally, Chem Draw Ultra (CDU 12.0) was utilized to construct the ligands and optimize their energy using the MM2 force field, ultimately saving them in pdb format. In silico docking studies of ligands against duplex DNA were thoroughly conducted using the Lamarckian Genetic Algorithm (LGA), which was extensively utilized to predict binding modes and conformations [30–33]. The grid maps for the docking simulations were positioned at the active site pocket of the protein targets, measuring 80x60x120 points with a grid-point spacing of 0.378 $Å^3$. Furthermore, BIOVIA software was employed to view and display the conformations [34].

2.2. Synthesis of 1–5 QSHSB ligands

1 mmol, (0.224 g) of quinoline-8-sulfonohydrazide and 1.1 mmol of the corresponding aldehyde were dissolved in 20 ml of absolute ethanol then subjected to gently stirring refluxed for 4 h. The solution was cooled, and the formed crystals were filtered and washed twice-using 20/20 ml diethyl ether and *n*-hexane.

The QSHSB's high purity was achieved through one to two recrystallization processes using a dichloromethane/hexane solvent mixture. The purity was further confirmed using silica gel thin-layer chromatography, which displayed a single spot using a mobile phase of hexane/ethyl acetate (70:30, *v*/v).

1: Yield: 90 % white crystals with m.*p* = 210 °C. MS (*m/z*) = 345.0 (theor. 345.9), Elemental Anal. Exp. (theor.%): C: 55.55 (55.57), H: 3.54 (3.50), and N: 12.11 (12.15 %) of general formula $C_{16}H_{12}ClN_3O_2S$. IR (cm^{-1}): 3280, m ($\nu_{N\text{-}H}$ stretch), 1610, m ($\nu_{C=N}$), 1577 and 1430 w ($\nu_{C=C}$), 1540, w ($\nu_{N\text{-}H}$ bend): 1230, m ($\nu_{N\text{-}C}$). ^{1}H NMR ($CDCl_3$, 400 MHz) δ (ppm): δ 7.21 (2H, dd, J = 7.6, 1.8 Hz), 7.51 (2H, dd, J = 8.2, 1.4 Hz), 7.75 (2H, dd, J = 8.3, 1.3 Hz),8.0–8.30 (3H, m (overlap broadband)), 8.36 (1H, s, HC═N), 8.95 (1H, d, J = 7.8 Hz, HC_{ph} = N), 12.02 (H, s, HN-N=C). δ ^{13}C NMR (ppm): δ 117.5–140.6 (14C, Aromatic-C), 142.4 (1C, N-N=C), 149.6 (1C, C_{ph} = N).

2: Yield: 88 % yellowish crystals m.*p* = 215 °C. MS (*m/z*) = 388.9 (theor. 390.4), Elemental Anal. Exp. (theor.): C: 49.04 (49.24), H: 3.05 (3.10), and N: 10.56 (10.77 %) of general formula $C_{16}H_{12}BrN_3O_2S$. IR (cm^{-1}): 3198, m ($\nu_{N\text{-}H}$ stretch), 1621, m ($\nu_{C=N}$), 1582 and 1428 w ($\nu_{C=C}$), 1538, w ($\nu_{N\text{-}H}$ bend): 1227, m ($\nu_{N\text{-}C}$). ^{1}H NMR ($CDCl_3$, 400 MHz) δ 7.42 (2H, dd, J = 7.3, 1.5 Hz), 7.58 (2H, dd, J = 8.3, 1.6 Hz), 7.88 (2H, dd, J = 7.9, 1.7 Hz), 8.1–8.28 (3H, m (overlap broadband)), 8.38 (1H, s, HC_{ph} = N), 9.02 (1H, d, J = 7.6 Hz), 12.20 (H, s, HN-N=C). ^{13}C NMR: δ 118–140 (14C, Aromatic-C), 142.51 (1C, N-N=C), 149.54 (1C, C_{ph} = N),

3: Yield: 68 % yellowish crystals m.*p* = 138–142 C°. MS (*m/z*) = 317.0 (theor. 317.8), Elemental Anal. Exp. (theor.): C: 52.84 (52.98), H: 3.35 (3.49), and N: 13.16 (13.24 %) of general formula $C_{14}H_{11}N_3O_2S_2$. IR (cm^{-1}): 3280, m ($\nu_{N\text{-}H}$ str:etch), 1610, m ($\nu_{C=N}$), 1577 and 1430 w ($\nu_{C=C}$), 1540, w ($\nu_{N\text{-}H}$ bend): 1230, m ($\nu_{N\text{-}C}$). ^{1}H NMR ($CDCl_3$, 400 MHz): δ 7.06 (2H, d, J = 7.5 Hz), 7.42 (1H, d, J = 5 Hz), 7.70–8.27 (5H, m (overlap broadband)), 8.39 (1H, s, HC_{ph} = N), 8.97 (1H, d, J = 7.8 Hz), 12.05 (H, s, HN-N=C). ^{13}C NMR: δ 117.5–144.4 (13C, Aromatic-C), 149.6 (1C, C_{ph} = N).

4: Yield: 85 % orange-red crystals m.*p* = 195–200 C°. MS (*m/z*) = 343.1 (theor. 343.9), Elemental Anal. Exp. (theor.): C: 55.87 (55.97), H: 3.35 (3.228), and N: 12.20 (12.24 %) of general formula $C_{16}H_{13}N_3O_4S$. IR (cm^{-1}): 3280, m ($\nu_{N\text{-}H}$ stretch), 1610, m ($\nu_{C=N}$), 1577 and 1430 w ($\nu_{C=C}$), 1540, w ($\nu_{N\text{-}H}$ bend): 1230, m ($\nu_{N\text{-}C}$). δ 6.73 (1H, d, J = 8.8 Hz), 7.23 (1H, d, J = 2 Hz), 7.42 (1H, d, J = 8.5 Hz), 7.73–8.29 (5H, m (overlap broadband), 8.47 (1H, s, HC═N), 9.05 (1H, d, J = 7.5 Hz), 11.64 & 11.92 (2H, 2 s, 2 HO-Ph), 12.12 (H, s, HN-N=C,). ^{13}C NMR: δ 113–141 (12C, Aromatic-C), 142.2 (1C, N-N=C), 145.9 & 147.8 (2C, Phenol Cs), 149.7 (1C, C_{ph} = N).

5: Yield: 94 % yellow crystals m.*p* = 235–240 C°. MS (*m/z*) = 378.2 (theor. 377.1), Elemental Anal. Exp. (theor.): C: 55.87 (63.65), H: 3.35 (4.01), and N: 11.13 (12.24) (%) of general formula $C_{20}H_{15}N_3O_3S$. IR (cm^{-1}): 3280, m ($\nu_{N\text{-}H}$ stretch), 1610, m ($\nu_{C=N}$), 1577 and 1430 w ($\nu_{C=C}$), 1540, w ($\nu_{N\text{-}H}$ bend): ^{1}H NMR ($CDCl_3$, 400 MHz) δ (ppm): δ 6.85 (1H, d, J = 8.6 Hz), 7.66 (2H, d, J = 8.6 Hz), 7.82–8.29 (7H, (overlap multiband), 8.32 (1H, s, HC═N), 9.15 (1H, d, J = 7.5 Hz), 11.64 (1H, s, HO-Ph), 12.06 (1H, s, HN-N=C). ^{13}C NMR: δ 115–140 (17C, Aromatic-C), 149.56 (1C, C_{ph} = N), 158.92 (1C, N-N=C), 166.23 (1C, Phenol C).

2.3. Antibacterial tests

The bacterial strains were purchased from the American Type Culture Collection (ATCC). The bacteria used in this study were *Bacillus subtillus (ATCC 6633)*, *Escherichia coli (ATCC25922)*, *Klebsiella pneumoniae (ATCC 13883)*, *Proteus vulgaris (ATCC 8427)*, *Pseudomonas aeruginosa (ATCC 9027)*, and *Staphylococcus aureus (ATCC 6538P)*, and *Staphylococcus epidermis (ATCC 12228)*. Moreover, *Staphylococcus aureus* isolated from clinical specimen showed vancomycin resistant. The broth turbidity of the isolated bacteria was standardized to a value of 0.5 McFarland (1.5 × 108 CFU/mL). Subsequently, the solution was mixed with normal saline to achieve a concentration of 1 × 107 colony-forming units per milliliter (CFU/mL).

2.4. Antibacterial susceptibility

Antibacterial susceptibility was performed using the disk diffusion susceptibility approach [35,36]. In summary, a standardized bacterial isolate with a concentration of 1.5 × 108 colony-forming units per milliliter (CFU/mL) was applied to the surface of Muller Hinton agar using a swab. Next, a circular 6 mm of diameter filter paper disks were soaked in a solution containing 0.1 mg/mL concentration of each of the compound. These disks were placed on the surface and incubated overnight at 37 °C. The diameters of the inhibition zones by the QSHSB compounds were measured.

2.5. Minimum bactericidal concentration (MBC) and minimum inhibitory concentration (MIC) determination

The antibacterial effectiveness against the preceding eight isolates was assessed by determining their minimum inhibitory concentration (MIC) and minimum bactericidal concentration (MBC) values [30]. The synthesized QSHSB (**1–5**) were diluted in a serial manner, with each dilution being twice as concentrated as the previous one, using Muller Hinton broth medium. Each dilution (1000, 500, 250, 125, 62.5, 31.25, 15.63, 7.81, 3.91, and 1.95 μg/mL) was cultured with 1 μL from a standardized bacterial isolated suspension containing 1 × 107 CFU/mL. Duplicates were made for each dilution. The two replicated wells were not inoculated, serving as a negative control. Subsequently, the other microplate wells had been treated with the inoculum and it was placed in an incubator (at 37 °C) overnight. MIC was determined as the lowest concentration of each compound that suppressed the growth of the tested isolate. Subsequently, the substances extracted from the wells because of MIC were applied in a linear pattern using sterile cotton swabs on nutrient agar plates that were devoid of antibacterial substances. The plates were then incubated at 37 °C overnight. MIC of each compound, which is the lowest concentration at which no bacterial growth was observed and considered as the minimum bactericidal concentration (MBC).

3. Results and discussion

3.1. Synthesis, EDX and MS

In an open environment reflux setting, the condensation of quinoline-8-sulfonohydrazide with 1:1 M ratio of the corresponding aldehyde in absolute ethanol solvent resulted in the formation of QSHSB desired ligands with significant yields (Scheme 1). In the synthesis of the QSHSB, the aldehyde was chosen over the ketone due to the typically prolonged dehydraction reaction to the Schiff base, which necessitated additional time and yielded a lower output; hence, it was excluded from this study, so constraining the preparation methodology. The novel QSHSB possesses a solid state as mainly white-yellow powder and displaying good solubility in CH_2Cl_2, DMSO and DMF, low solubility in H_2O and ROH, and insoluble in ethers or n-hexane.

The molecular and structural formulas of **1–5** QSHSB were determined through the utilization of MS, CHN, NMR, TGA, FT-IR, and UV–Visible spectroscopic techniques.

3.2. QSHSB molecular hybrid design (MHD)

The concept of compound hybrid design involves connecting multiple molecules that contain numerous functional groups with atoms that have lone pair electrons and a specific biological activity [37]. This connection is achieved through a straightforward reaction, resulting in creation of novel hybrid poly-functional group compounds [37–39]. The purpose of this design is to enhance the pharmaceutical activity, medical capacity, stability, or eliminate undesirable physical or biological properties of these compounds. Here, three pharmacophoric units were meticulously included by the QSHSB MHD: An electron-dense heterocycle framework based on quinoline (**1–5**) can intercalate DNA and prevent bacterial topoisomerase. Polydentate complexation with electrophilic centers is possible, donor-acceptor H-bond sources are available, and conformational adaptability for ligand binding is enabled by the sulfonyl hydrazone bridge. Aldehyde moieties incorporate aromatic rings to augment π-π stacking with nucleobases, while electron-withdrawing groups (4-Cl/Br with highly electronegative elements in

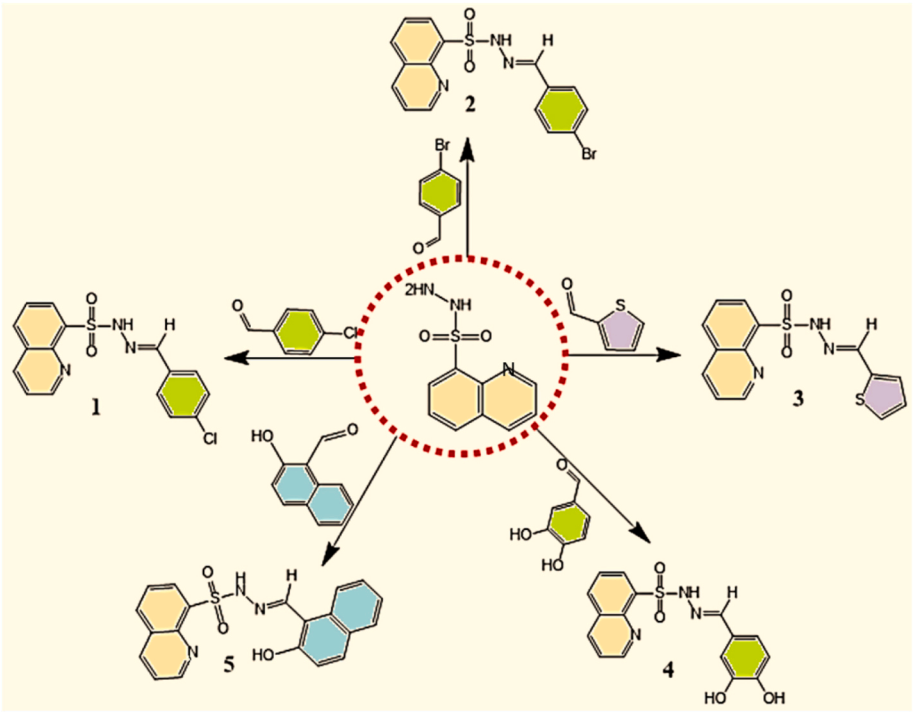

Scheme 1. Synthesis of **1–5** QSHSB ligands.

1–2) are introduced to increase the polarity of the compounds. Thiophene in **3** was utilized to enhance hydrophobic interaction combinations. The phenolic group, as seen in **4–5**, is examined for its ability to construct H-bonds with DNA, particularly with the its phosphate functional group.

The approach entails the synthesis of a single molecule fulfilled the Ro5 pharmacokinetic rules through combining the quinolone and hydroxyl-naphthal pharmacophores via sulfonylhydrazone bridge (Fig. 1), for developing a new antibacterial agent and novel 1BNA binder molecules.

In subsequent research, the QSHSB compounds can be assessed as poly-chelate ligands due to their abundance of e-rich atoms and their anticipated ability to form tetra-dentate coordination complexes with transition elements. Furthermore, the QSHSB and their complexes will be assessed as compounds exhibiting anticancer properties.

3.3. EDX, CHN and MS analysis

CHN-elemental, MS and EDX analysis of the **1–5** QSHSB ligands were in agreement with their proposed molecular formula and atomic continent (see exp. part). For example, ligand **2** MS and EDX analysis have been illustrated as atypical example in Fig. 2. The MS was agreed with the M.Wt: $m/z = 388.5$ [M^+] (theo. $m/z = 388.8$) as shown in Fig. 2a. In addition, EDX analysis Fig. 2b proved the atomic composition and purity of ligand **2**, and the spectrum indicated the existence of just C, O, N, Br and S sited to their expected energy signals, that corresponds to the empirical formula of this ligand.

3.4. Ft-IR

The FT-IR measurement was used here for two aspects: the first is to supplement the dehydration reaction by monitoring the vibration changes of the functional groups in the reactants and comparing with the product, and the second is to prove the formation of the **1–5** QSHSB ligands. In order to achieve the first goal, the formation of ligand **1** was taken as reaction model. Fig. 3 presents a comparison of the FT-IR spectra of quinoline-8-sulfonohydrazide and 4-chlorobenzaldehyde, and ligand **1**. The foundation of **1** was justified by the following noteworthy indicators: the stretching vibration of N—H_2 in quinoline-8-sulfonohydrazide at 3365 cm^{-1} was totally disappeared, parallel to downfield shifting of the N—H peaks at 3285 and 3244 cm^{-1} to 3105 and 3085 cm^{-1} respectively. Finally, the stretching frequency of the C═O bond in 4-chlorobenzaldehyde at 1689 cm^{-1} also was dropped to 1623 cm^{-1}. All these seen, evidenced the dehydration of H_2O from hydrazide and aldehyde to develop the C═N functional group in **1**. Moreover, in the **1–5** ligands FT-IR spectra showed similar vibration behaviors, the main characteristic bands at 3110–3080, 3000–2980, 1660–1580, 1350–1180 cm^{-1} can be attributed to $\nu_{N\text{-}H}$, $\nu_{C\text{-}H}$, $\nu_{C=N}$ and ν_{SO2} functional group, respectively (Fig. 3), such values fitted with QSHSB recent reported FT-IR data [40,41].

3.5. UV–Vis. And optical activities

The UV–Visible properties of **1–5** QSHSB ligands in addition of condensation targeting of reaction were carried out in dichloromethane within the 240–550 nm range. Synthesis pathway of ligand **3** was chosen as a specific example in order to follow up the imidization reactions. Absorption measurements were used to prove the occurrence of the dehydration reaction by tracking the behavior of both the thiophene-2-carbaldehyde and quinoline-8-sulfonohydrazide before and after condensation together (Fig. 4b). A significant disparity in the UV-behavior was recorded when **3** was formed as shown in Fig. 4a, since the number, shape and location of the Uv-signals have been changed, this proved that the desired reaction has been occurred. In general, the desired five ligands reflecting various absorbance behavior, for **1** and **2** reflected a very similar behavior, both have close $\lambda_{max} = 314$ and 310 nm, respectively, **3** and **4** showed two bands for both, $\lambda_{max} = 272$ and 343 nm for **3**, and $\lambda_{max} = 276$ and 318 nm for **4**. Moreover, **5** has more complicated UV-spectrum, one shoulder at 262 nm band with $\lambda_{max} = 333$ nm, and a broadband with $\lambda_{max} = 414$ nm with two shoulders at 434 and 390 nm. All those e-transfer bands can be attributed to π–π^* and/or n–π^* types.

The direct experimental ΔE_g of each QSHSB ligands were determined via Tauc's Eq. [42], this equation is the best well-known method to estimate the optical energy gap for materials. The direct bandgap values for **1–5** were found as 4.21, 4.18, 3.21, 3.52, and 2.75 eV, respectively, as shown in Fig. 4c. As a result, the desired ligands can be categorized as a broad bandgap semiconductor (HBSC). This experimental methodology provides a thorough comprehension of the ligand's electronic characteristics while it interacts with the solvent. It is particularly useful when the direct optical energy gap is greater than 4 eV. The highly synthesized QSHSBs have large bandgaps (2.75–4.21 eV), as a result, it is well suited for potential applications in optoelectronics, solar cells, sensors and power electronics. This is due to the extensive possibilities

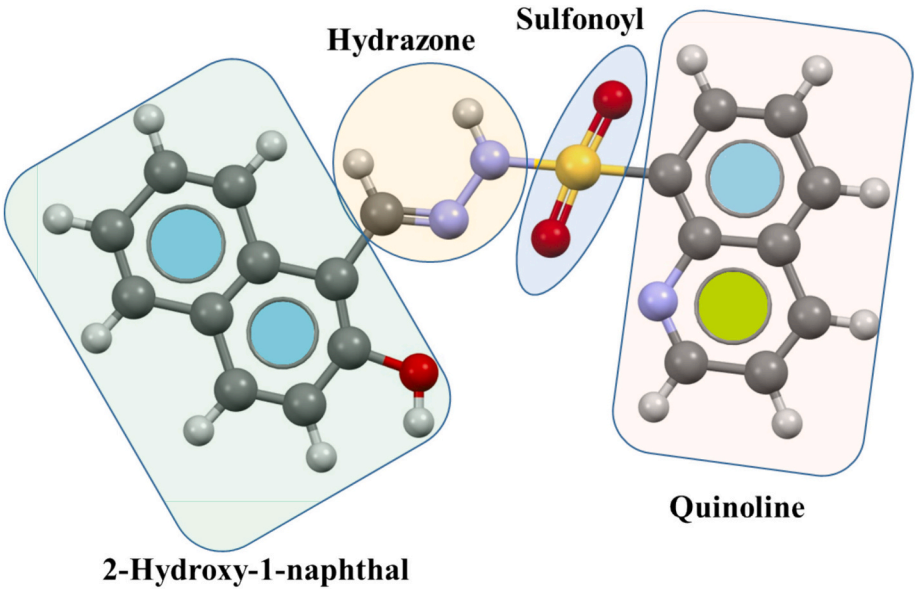

Fig. 1. MHD schematic of ligand **5** as QSHSB hybrid compound.

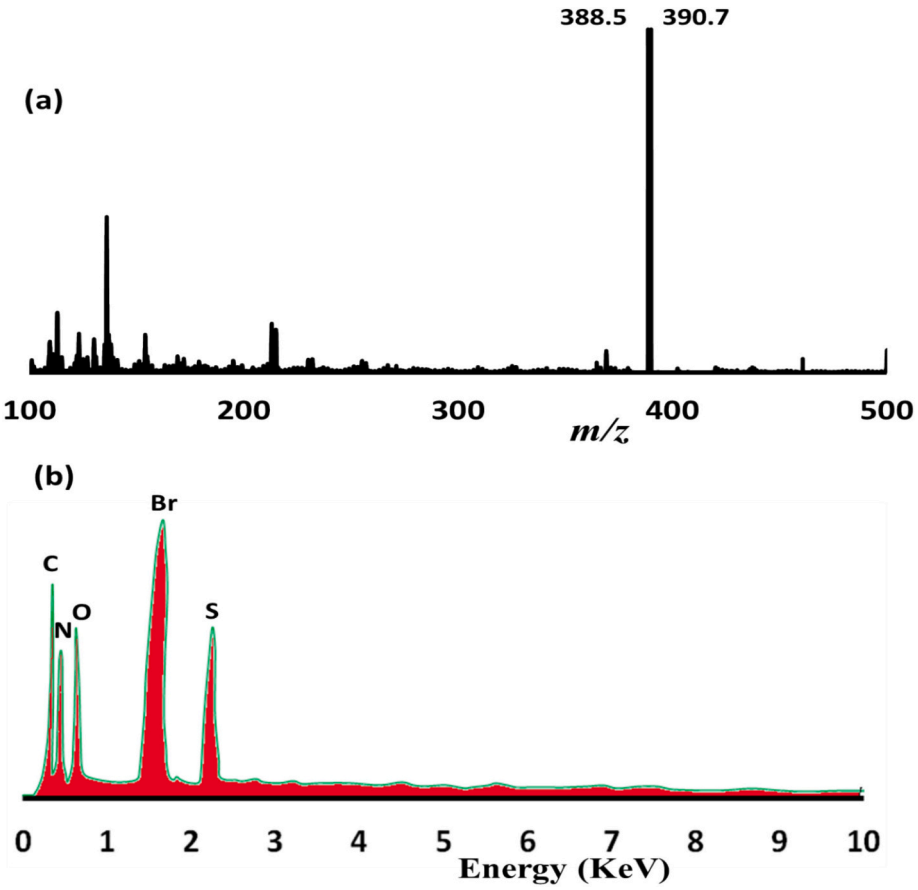

Fig. 2. (**a**) MS and (**b**) EDX of **2** QSHSB.

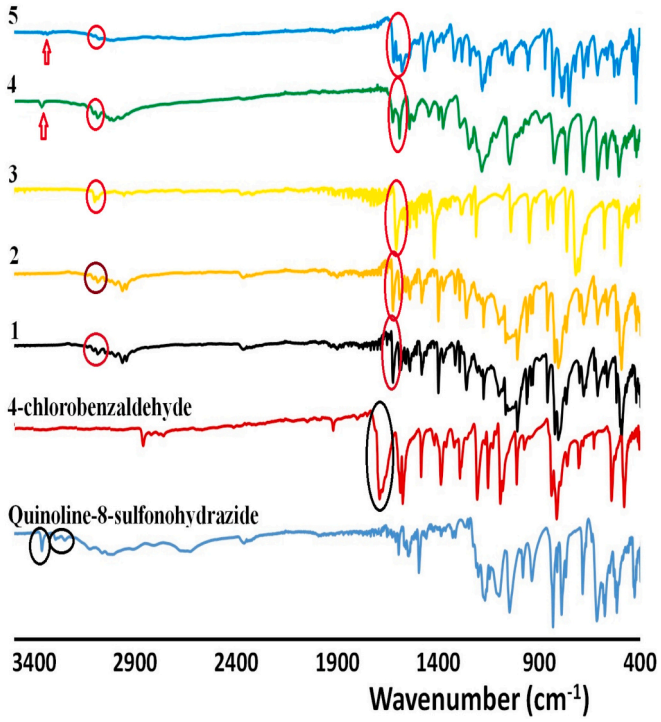

Fig. 3. QSHSB (**1–5**) FT-IR investigations.

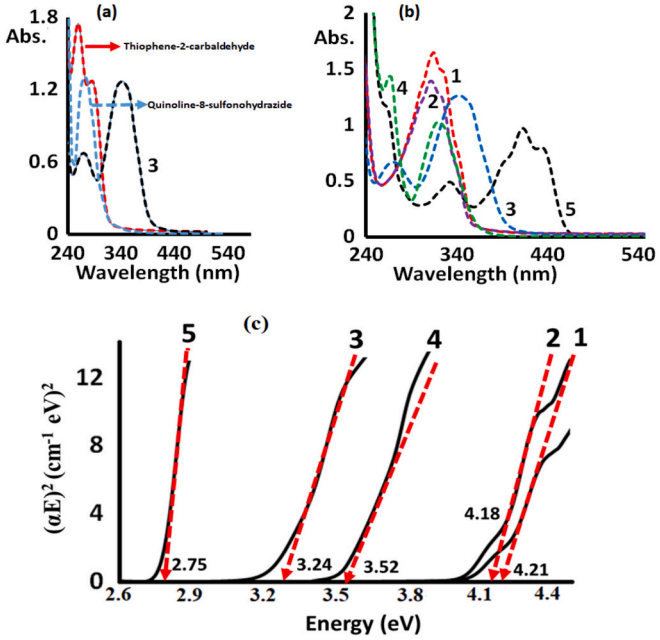

Fig. 4. (a) UV-monitoring of **3,** (b) UV–Vis. and (c) Tauc's ΔE_g of **1–5** QSHSB ligands.

offered by wide bandgap semiconductors [41–43].

3.6. NMR

The ^{1}HNMR data for the **1–5** QSHSB ligands were obtained in $CDCl_3$; all the compounds reflected signals only in the aromatic region since no aliphatic proton or carbon are used in both quinoline-8-sulfonohydrazide and functionalized aldehydes used in the synthesis of the desired ligands. As atypical example, ligand **5** NMR result was illustrated in Fig. 5. The displayed ^{1}HNMR spectrum (Fig. 5a) showed a singlet peak at 12.06 ppm that due to the N—H amidic proton, the phenolic (O—H) proton appeared as singlet peak at 11.64 ppm. Also, the chemical shift of (N=CH) the azomethine proton appeared as singlet peak at 8.32 ppm, the N-CH proton of quinoline appeared as doublet peak at 9.15 ppm, and all the other aromatic protons appeared in the area range 6.85–8.29 ppm.

Due to the absence of aliphatic carbons in ligand **5**, the ^{13}C NMR spectra was adjusted to a range of 90–200 ppm. Consequently, all the carbons were observed within the 110–170 ppm region (Fig. 5b). Therefore, due to the fact that all carbons were aromatic, it was imperative to employ the DEPT ^{13}C NMR technique to differentiate between types between C, CH, CH_2 and CH_3 carbon types, where C and CH_2 appear with upward signs, while CH and CH_3 appear with downward signs. Due to the absence of CH_2 or CH_3 in ligand **5**, it was straightforward to distinguish between C and CH carbon types using information on the ^{13}C chemical shift values. To facilitate this task, the signals were numbered with their corresponding carbons directly on the spectra, taking into consideration that some signals can be determined based on the carbon chemical environment. For example, C1 (*o*-phenyl, CH) 115.5 ppm, C2 (HO-C phenyl, C) =164.6 ppm, C3 (N=CH, CH) 159.1 ppm, and C4 (o-Py, CH) 148.9 ppm. All the other carbons were cited to their positions according to their sign's direction as well as their expected chemical shifts (Fig. 5b).

3.7. TG/DTG

The TG/DTG behaviors of the ligands **1–5** were studied throughout a temperature range from 25 to 1000 °C, with 5 °C. min^{-1} heating rate

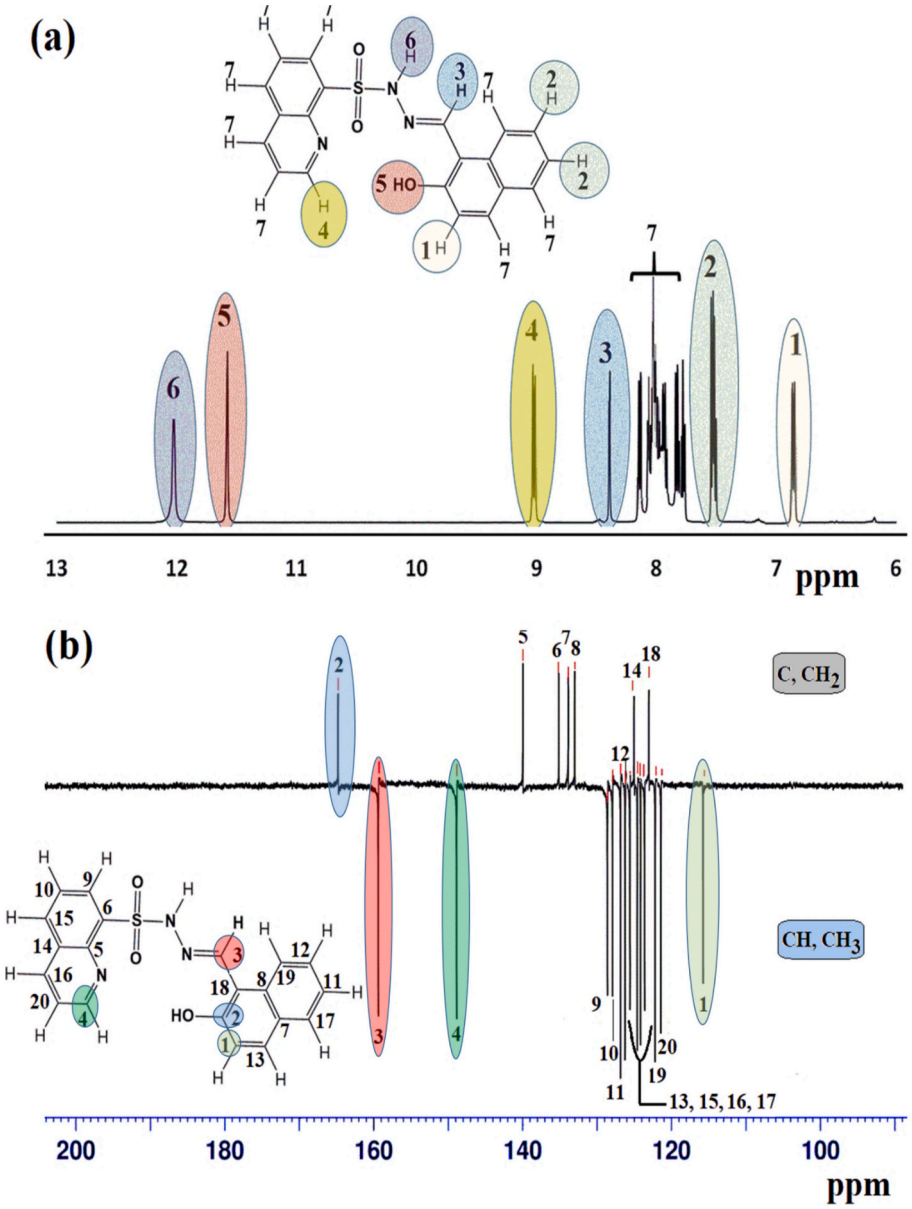

Fig. 5. (a)^{1}H, and (b)^{13}C NMR of **5** in $CDCl_3$.

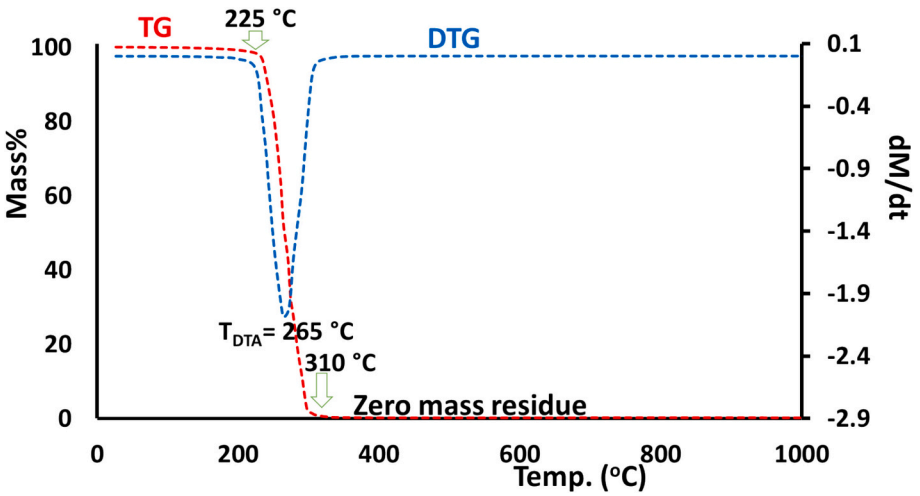

Fig. 6. TG/DTG of ligand **5**.

under open ambient condition. All the **1–5** QSHSB ligands showed similar one-step thermal decomposition behavior, as the ligand **5** was showed the highest thermal stability; its TG/DTG was taken as typical example (Fig. 6). The stability of ligand **5** was observed up to around 225 °C, with no detectable mass loss reflecting not only the stability of **5** but also the absence of any impurities, including the water moisture or solvents remaining in the ligand lattice. However, at temperature over 230 °C, the molecule began to breakdown in one stage and ended up at 310 °C with a decomposition temperature T_{DTA} = 265 °C. Moreover, the pure **5** underwent full breakdown with approximately 100 % mass loss, resulting in the production of light gases such as CO, CO_2, NOx, and SOx [44], which was evident by zero_mass_residue above 310 °C as seen in Fig. 6.

3.8. Bioinformatics study

3.8.1. Ro5

The Ro5 bioinformatics analysis were carried out to investigate the drug-like properties of QSHSB **1–5** ligand. The **1–5** exhibited favorable drug-likeness model scores and promising physicochemical characteristics, as per Lipinski's (Ro5) rule of five [45]. **1–5** ligands under investigation possessed hydrogen bond acceptors (HBA), hydrogen bond donors (HBD), the molecular weights; the value of the rotatable bonds (nrotb) was also investigated. Furthermore, the Log *P* values of each ligands (Table 1). Consequently, the recent QSHSB ligands exhibited potential as drug-like candidates, meeting the criteria of having a of M. Wt of 315–390, a Log P value of 2.3–4, a maximum of 1–3H-bond acceptors (HBA), a maximum of 4–6H-bond donors (HBD), and a 4 rotatable bonds (nrotb) [46–48].

3.8.2. 1BNA-docking

Molecular docking – In Silico - is widely recognized technique for identifying potential lead candidates that can specifically bind to preferred binding sites in nucleic acids or protein receptors. In addition, it allows for the exploration of various noncovalent interactions between the pro-drug and the receptor. The chemotherapeutic actions of Schiff base chelated ligands have attracted the attention of numerous academic and clinical scientists, since ligands of this nature are commonly having the ability to interact with DNA, which is the main target of anticancer drugs within cells [49]. In this study, a molecular docking analysis was performed to determine the binding affinity of **1–5** with the active site residues of 1BNA. Overall, the ligands **1–5** QSHSB demonstrated superior binding capabilities, as indicated by the docking energy range of −8.0-11.0 kcal/mol. These ligands fit well into the curved

Table 1
In silico **Ro5** pharmacokinetic properties of **1–5.**

QSHSB	M. Wt.	Log P	HBA	HBD	Nrotb	Ro5 drug-Likeness
1	345.9	3.73	1	4	4	M.Wt. ≤ 500, LogP≤4.15, HBA ≤ 10 and HBD ≤ 5, Nrotb≤10.
2	388.9	3.99	1	4	4	
3	317.0	3.09	1	5	4	
4	343.1	2.33	3	6	4	
5	378.2	3.84	2	5	4	

Table 2
1BNA docking result with **1–5** QSHSB ligand.

No.	B.E (kcal/mol)	L. E	I. C μM T = 298.15 K	RMSD (Å)	Hb of residues and ligands with bond length (Å)
1	−9.81	−0.39	10.73	1.4	DNA:A:DG4:H22……O (1.850) DNA:B:DG22:H3……O (1.904) DNA:B:DG22:H22….N (2.057) DNA:A:DG10:H21……S (1.888)
2	−10.07	−0.44	11.26	1.1	DNA:A:DG10:H3…….O (2.116) DNA:B:DG16:H22……O (2.076) DNA:B:DG16:H3…….N (2.019) DNA:A:DG10:H21……O (2.083)
3	−8.91	−0.27	9.71	2.2	DNA:B:DG16:H3…….O (1.989) DNA:B:DG16:H22……S (1.596) DNA:A:DG10:H21……N (2.075)
4	−9.36	−0.37	10.25	1.7	DNA:A:DG12:H3…….O (1.758) DNA:B:DG16:H22……O (1.979) DNA:B:DG16:H3…….O (1.761) DNA:A:DG4:H3……..N (2.025)
5	−8.22	−0.23	9.54	2.3	DNA:B:DG22:H22……O (2.101) DNA:B:DC23:H1……..O (2.139)

I·C: Inhibition Constant, B.E: Binding Energy, L.E: Ligand Efficiency, VdW: Vander Walls energy, Des: Dissolve energy.

structure of the DNA target and mostly bind to the minor groove. The docking analysis indicates that DNA forms strong bonds with ligands**1–5** mostly by typical hydrogen bonding, π-alkyl, Van der Waals, and π-sulfur hydrophobic interactions, as listed in Table 2. In general, scoring the ligands depending on the binding energy as follows **2** > **1** > **4** > **3** > **5**, therefore, **2** was selected as the representative example for discussing the binding results, due to its superior binding capacity compared to the other ligands (Fig. 7a) demonstrated that **2** with minor groove binding mode and as DNA double helix binder like the others (Fig. 7b) with highest docking score = −10.07 kcal/mol (Table 2). Fig. 7c showed four clear short hydrogen bond interactions demonstrated as DNA:A:DG10:H21…..S with 1.888 Å, DNA:A:DG10:H3….O with 2.116 Å, DNA:B:DG16:H22…..O with 2.076 Å, DNA:B:DG16:H3….N with 2.019 Å. Furthermore, exceptionally the bromide and sulfur (of SO_2) mostly contributed to the enhanced DNA-binding ability of **2** compared to the other QSHSB ligands, due to the existence of extra π-alkyl and π-sulfur hydrophobic interactions, respectively, as seen in Fig. 7d.

3.9. Anti-bacterial evaluations

The results in this study showed that the quinoline-8-sulfonohydrazide and **1–5** QSHSB ligands exhibited substantial promise as antibacterial agents, displaying promising effectiveness. The in vitro antibacterial activity screening of the investigated compounds was tested by agar disk diffusion method. Biologically, we intended to investigate a wider variety of bacteria, fungi and cancer cells; but, only seven types of bacteria are accessible in our laboratory. All the QSHSB displayed antibacterial activity against most tested bacterial isolates (Fig. 8a). The obtained results revealed that the studied compounds acted as antibacterial agents with variable effect. **3** showed antibacterial effect against both Gram-positive and Gram-negative isolates with an inhibition zone range (10–13 mm).

The antibacterial activity was further evaluated through the measurement of the MIC and MBC values using micro-broth dilution method. The obtained results demonstrated that all QSHSB **1–5** ligands possess antibacterial inhibitory activity against the tested bacterial isolates with some variation in their effective working concentrations (Fig. 8b). The obtained MIC results indicated that **3** was the highest effective, since it inhibited the growth of all tested bacterial isolates at concentrations within the 62.5 μg/mL to 125 μg/mL range. Moreover, **5** inhibited the growth of all examined Gram-negative bacterial isolates, with MIC values ranging from 7.8125 μg/mL to 250 μg/mL. In this work, the examined isolate *S. epidermis* was responsive to the inhibitory action of **3** with MIC value of 125 μg/mL which is equal to the MIC value of Gentamicin. In addition, *P. vulgaris* and *P. aeruginosa* were the most sensitive to **5**, with MIC values of 62.5 μg/mL and 7.8125 μg/mL, respectively. Besides MIC determination, MBC measurements for all compounds were also investigated (Fig. 8c). The MBC results revealed that **3** worked as bactericidal agent at a concentration range from 125 μg/mL to 500 μg/mL against all tested bacteria. Furthermore, **5** acted as bactericidal agent against *P. aeruginosa* at 62.5 μg/mL concentration.

Comparing the biological results obtained in this study with those of their equivalents [50–53] revealed a significant degree of convergence, particularly in the antibacterial aspect, where IZD in this study was determined to be 10–13 mm compared to 12–14 mm, furthermore, the Schiff base/M complexes exhibited superior antibacterial activity compared to the free Schiff bases [53]. In terms of DNA binding, compound **5** (in this investigation) exhibited marginally superior DNA binding, presumably due to the formation of a significant number of hydrogen bonds with the DNA.

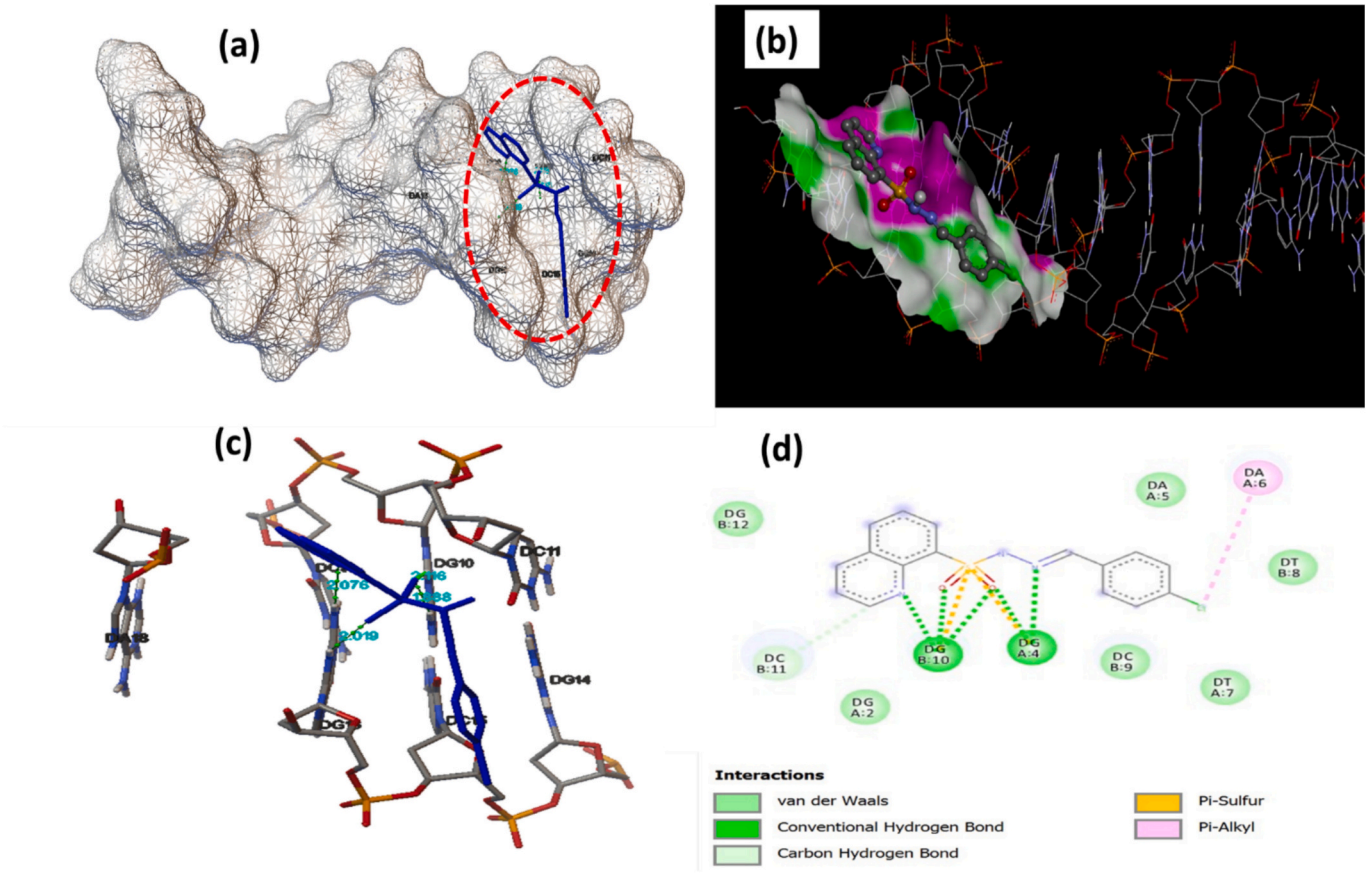

Fig. 7. Docking result of **2**: (a) minor groove binding, (b) double-helix interactions, (c) H-bonds interactions and (d) 2D showing all the interactions.

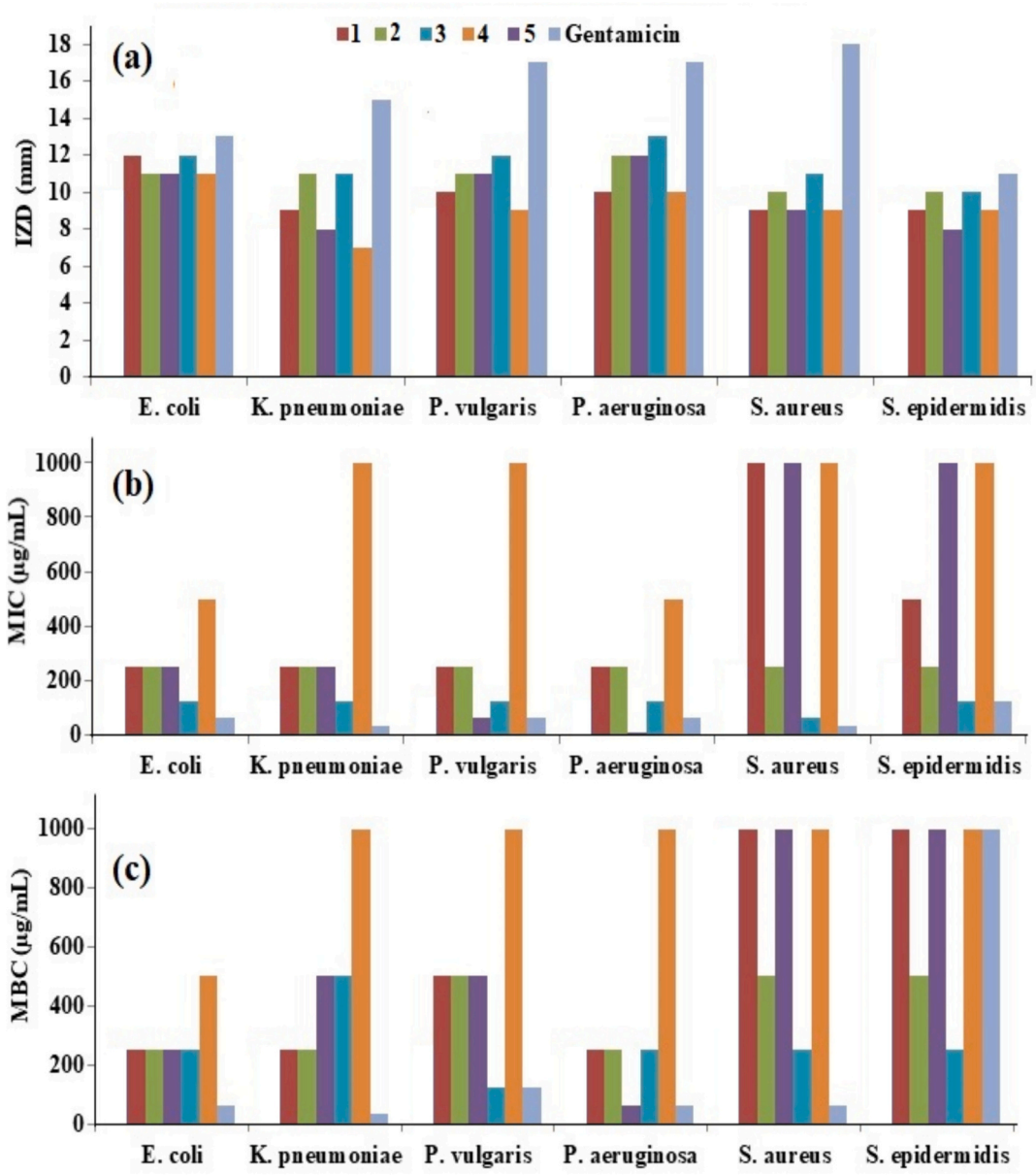

Fig. 8. QSHSB (**1–5**) antibacterial activity via (a) IZD, (b) MIC, and (c) MBC.

3.10. Structure-activity relationship (SAR) of 1–5 QSHSB

The synthesized QSHSB derivatives (**1–5**) exhibit distinctive structural features that substantially influence their physicochemical and biological properties. The results highlight that targeted modifications to the verified aldehyde group and fixed quinolone and sulfonyl hydrazone core pharmacophores could enhance antibacterial and DNA-binding efficacy.

First of all, **1–5** conform to Lipinski's Rule of Five (Ro5) (M.Wt. < 500, LogP = 2.3–4.0, HBD ≤ 5, HBA ≤ 10) as seen in Table 1, ensuring favorable drug-likeness and oral bioavailability [45,48]. Ligand **3** (LogP = 3.09) attains an optimal balance between hydrophobicity and solubility, facilitating efficient membrane penetration while maintaining bioavailability [47]. The sulfonyl hydrazone bridge (–SO_2–NH–N=CH–) is essential for the bioactivity of the ligands. The adaptable conformation enhances optimum binding to the DNA minor groove (Fig. 7a), as confirmed by molecular docking analyses (Table 2). This bridge serves as an essential hydrogen bond donor and acceptor, enhancing interactions with DNA (e.g., ligand **2** formed four hydrogen bonds with 1BNA) [28,31]. The bridge improves thermal stability for all ligands, making them suitable for medical applications [44]. The quinoline core is essential for π-stacking interactions, promoting DNA intercalation and stabilizing ligand-DNA complexes (Fig. 7) [20,23].

The substituents produced from aldehydes (varied across **1–5**) profoundly impact biological activity: Electron-withdrawing groups: Ligand **1** (4-Cl) and Ligand **2** (4-Br) exhibit notable antibacterial activity, with Ligand **2** displaying the greatest DNA-binding affinity (−10.07 kcal/mol). The bromine atom enhances hydrophobic (π-alkyl/π-sulfur) interactions and hydrogen bonding, whereas the electron-withdrawing group effect increases C=N electrophilicity, hence improving interactions with bacterial enzymes and DNA [21,50].

The thiophene moiety (Ligand **3**) demonstrates the broadest range of action (MIC = 62.5–125 µg/mL), attributed to enhanced hydrophobicity and π-stacking, which facilitate membrane penetration and target binding [37].

Phenolic groups (Ligands **4–5**): Ligand **5** (mono-hydroxy) exhibits significant activity against *P. aeruginosa* (MIC = 7.81 µg/mL), likely due to hydrogen bonding between the phenolic –OH and the phosphate

backbones of bacterial DNA [22,52].

4. Conclusion

Five new quinoline-sulfonohydrazide Schiff base (QSHSB) ligands were produced in high yields by a simple condensation reaction involving quinoline-8-sulfonohydrazide and various aldehydes. The formation and purity of the QSHSB derivatives (**1–5**) were meticulously validated by a comprehensive array of analytical techniques, including FT-IR, UV–Vis, $^{1}H/^{13}C$ NMR, MS, EDX, and CHN elemental analysis. TGA/DTG reflected the QSHSB ligands with remarkable stability (up to 225 °C) and one step decomposition process. The novel QSHSB were synthesized in significant yields with semiconductor-like optical properties with wide bandgaps (2.75–4.21 eV) suitable for optoelectronic applications. The Molecular Hybrid Design (MHD) methodology employed to develop the QSHSB ligands effectively incorporated three pharmacophoric components—quinoline, a sulfonyl hydrazone linkage, and aldehyde-derived substituents—all are chosen to fulfil the Lipinski's (Ro5) and enhance the 1BNA DNA docking result. Therefore, **2** was identified as the most effective DNA binder, exhibiting a docking binding energy of −10.07 kcal/mol and establishing many hydrogen bonds as well as π-π/π-sulfur interactions with minor groove interaction. Additionally, antibacterial assays (IZD, MIC, and MBC) demonstrated significant efficacy against both Gram-positive and Gram-negative pathogens. **3** demonstrated broad-spectrum inhibitory and bactericidal effects (MIC = 62.5–125 μg/mL), whereas **5** showed significant bactericidal activity, especially against *Pseudomonas aeruginosa* (MIC = 7.81 μg/mL), indicating potential therapeutic significance.

Research ethics committee

The Research Ethics Committee has reviewed and approved current research proposal.

CRediT authorship contribution statement

H. Qrareya: Formal analysis, Data curation. **S. Sadi:** Formal analysis, Data curation. **L. Abdallah:** Investigation, Formal analysis. **A. Zarrouk:** Software, Resources. **F. Al battah:** Formal analysis, Data curation. **I. Warad:** Formal analysis, Data curation.

Consent for publication

Not applicable.

Declaration of competing interest

The authors declare no competing interests.

Acknowledgements

Qrareya. H. thanks the Arab American University-Palestine (AAUP) logistic support.

Data availability

No data was used for the research described in the article.

References

[1] X. Liu, J.R. Hamon, Recent developments in penta-, hexa- and hepta-dentate Schiff base ligands and their metal complexes, Coord. Chem. Rev. 389 (2019) 94, https://doi.org/10.1016/j.ccr.2019.03.010.
[2] M. Kaur, S. Kumar, M. Yusuf, J. Lee, R.J.C. Brown, K.H. Kim, A.K. Malik, Post-synthetic modification of luminescent metal-organic frameworks using Schiff base complexes for biological and chemical sensing, Coord. Chem. Rev. 449 (2021) 214214, https://doi.org/10.1016/j.ccr.2021.214214.
[3] A. Sakthivel, K. Jeyasubramanian, B. Thangagiri, J.D. Raja, Recent advances in Schiff base metal complexes derived from 4-aminoantipyrine derivatives and their potential applications, J. Mol. Struct. 1222 (2020) 128885, https://doi.org/10.1016/j.molstruc.2020.128885.
[4] W.A. Zoubi, A.A.S.A. Hamdani, M. Kaseem, Synthesis and antioxidant activities of Schiff bases and their complexes, Appl. Organomet. Chem. 30 (10) (2016) 810, https://doi.org/10.1002/aoc.3506.
[5] A. Catalano, M.S. Sinicropi, D. Iacopetta, J. Ceramella, A. Mariconda, C. Rosano, E. Scali, C. Saturnino, P. Longo, A review on the advancements in the field of metal complexes with Schiff bases as antiproliferative agents, Appl. Sci. 11 (2021) 6027, https://doi.org/10.3390/app11136027.
[6] A. Carreño, L. Rodríguez, D.P. Hernández, R.M. Trasanco, C. Zúñiga, D.P. Oyarzún, M. Gacitúa, E. Schott, R.A. Pérez, J.A. Fuentes, Two new fluorinated phenol derivatives pyridine Schiff bases: synthesis, spectral, theoretical characterization, inclusion in epichlorohydrin-β-cyclodextrin polymer and antifungal effect, Front. Chem. 6 (2018) 312, https://doi.org/10.3389/fchem.2018.00312.
[7] S. Chen, X. Liu, X. Ge, Q. Wang, Y. Xie, Y. Hao, Y. Zhang, L. Zhang, W. Shang, Z. Liu, Lysosome-targeted iridium (III) compounds with pyridine-triphenylamine Schiff base ligands: syntheses, antitumor applications and mechanisms, Inorg. Chem. Front. 7 (2020) 91, https://doi.org/10.1039/C9QI01161G.
[8] H. Bahron, S.S. Khaidir, A.M. Tajuddin, K. Ramasamy, B.M. Yamin, Synthesis, characterization and anticancer activity of mono-and dinuclear Ni(II) and co(II) complexes of a Schiff base derived from o-vanillin, Polyhedron 161 (2019) 84, https://doi.org/10.1016/j.poly.2018.12.055.
[9] J.R. Morrow, K.A. Kolasa, Cleavage of DNA by nickel complexes, Inorg. Chim. Acta 195 (1992) 245, https://doi.org/10.1016/S0020-1693(00)85319-0.
[10] H.G. Aslan, S. Akkoç, Z. Kökbudak, Anticancer activities of various new metal complexes prepared from a Schiff base on A549 cell line, Inorg. Chem. Commun. 111 (2020) 107645, https://doi.org/10.1016/j.inoche.2019.107645.
[11] S. Mukherjee, J.W. Yang, S. Hoffmann, B. List, Asymmetric enamine catalysis, Chem. Rev. 107 (2007) 5471, https://doi.org/10.1021/cr0684016.
[12] D.J. Bhatt, G.C. Kamdar, A.R. Parikh, Studies on sulfonylhydrazones: preparation and antimicrobial activity of arylsulfonyl-(4-substituted)- aceto/propiophenone hydrazones, J. Indian Chem. Soc. 2 (1984) 788.
[13] N. Özbek, G. Kavak, Y. Özcan, S. İde, N. Karacan, Structure, antibacterial activity and theoretical study of 2-hydroxy-1-naphthaldehyde-N-methylethanesulfonylhydrazone, J. Mol. Struct. 919 (2009) 154, https://doi.org/10.1016/j.molstruc.2008.09.010.
[14] R.J. Henry, The mode of action of sulfonamides, Bacteriol. Rev. 7 (1943) 175, https://doi.org/10.1128/br.7.4.175-262.1943.
[15] S.M. Sakya, X. Hou, M.L. Minich, B. Rast, A. Shavnya, K.M.L. DeMello, H. Cheng, J. Li, B.H. Jaynes, D.W. Mann, C.F. Petras, S.B. Seibel, M.L. Haven, 5-heteroatom substituted pyrazoles as canine COX-2 inhibitors. Part III: molecular modeling studies on binding contribution of 1-(5-methylsulfonyl) pyrid-2-yl and 4-nitrile, Bioorg. Med. Chem. Lett. 17 (2007) 1067, https://doi.org/10.1016/j.bmcl.2006.11.026.
[16] T.K. Sasikumar, L. Qiang, D.A. Burnett, D. Cole, R. Xu, H.M. Li, W.J. Greenlee, J. Clader, L. Zhang, L. Hyde, Tricyclic sulfones as orally active γ-secretase inhibitors: synthesis and structure–activity relationship studies, Bioorg. Med. Chem. Lett. 20 (2010) 3632, https://doi.org/10.1016/j.bmcl.2010.04.104.
[17] W.H. Cheung, S.L. Zheng, W.Y. Yu, G.C. Zhou, C.M. Che, Ruthenium porphyrin catalyzed intramolecular Carbenoid C− H insertion. Stereoselective synthesis of cis-disubstituted oxygen and nitrogen heterocycles, Eur. J. Org. Chem. (2005) 1479, https://doi.org/10.1021/ol034806q.
[18] V.K. Aggarwal, J. de Vicente, R.V. Bonnert, Catalytic cyclopropanation of alkenes using diazo compounds generated in situ. A novel route to 2-Arylcyclopropylamines, Org. Lett. 3 (2001) 2785, https://doi.org/10.1021/ol0164177.
[19] A.A. AlObaid, M. Suleiman, C. Jama, A. Zarrouk, I. Warad, Synthesis, physicochemical, optical, thermal and TD-DFT of (E)-N′-((9-ethyl-9H-carbazol-3-yl)-methylene)-4-methyl-benzene-sulfonohydrazide (ECMMBSH): naked eye and colorimetric Cu2+ ion chemosensor, J. King Saud Univ. Sci. 33 (2021) 101633, https://doi.org/10.1016/j.jksus.2021.101633.
[20] E. Lindner, H.A. Mayer, I. Warad, K. Eichele, Supported organometallic complexes, J. Organomet. Chem. 665 (2003) 176, https://doi.org/10.1016/s0022-328x(02)02112-5.
[21] S. Murtaza, S. Shamim, N. Kousar, M.N. Tahir, M. Sirajuddin, U.A. Rana, Synthesis, biological investigation, calf thymus DNA binding and docking studies of the sulfonyl hydrazides and their derivatives, J. Mol. Struct. 1107 (2016) 99, https://doi.org/10.1016/j.molstruc.2015.11.046.
[22] M.A. Salem, A. Ragab, A. El-Khalafawy, A.H. Makhlouf Ahmed, A. Askar, Y. A. Ammar, Design, synthesis, in vitro antimicrobial evaluation and molecular docking studies of indol-2-one tagged with morpholinosulfonyl moiety as DNA gyrase inhibitors, Bioorg. Chem. 96 (2020) 103619, https://doi.org/10.1016/j.bioorg.2020.103619.
[23] Y. Hu, G. Pan, Z. Yang, T. Li, J. Wang, M.F. Ansari, C. Hu, R.R.Y. Bheemanaboina, Y. Cheng, C. Zhou, J. Zhang, Novel Schiff base-bridged multi-component sulfonamide imidazole hybrids as potentially highly selective DNA-targeting membrane active repressors against methicillin-resistant Staphylococcus aureus, Bioorg. Chem. 107 (2021) 104575, https://doi.org/10.1016/j.bioorg.2020.104575.
[24] I. Warad, A.F. Eftaiha, M.A. Al-Nuri, A.I. Husein, M. Assal, A. Abu-Obaid, N. Al-Zaqri, T. Ben Hadda, B. Hammouti, Metal ions as antitumor complexes-review, J. Mater. Environ. Sci. 4 (2013) 542.
[25] F. Abu Saleemh, S. Musameh, A. Sawafta, P. Brandao, C.J. Tavares, S. Ferdov, A. Barakat, A. Al Ali, M. Al-Noaimi, I. Warad, Diethylenetriamine/diamines/copper

(II) complexes [Cu(dien)(NN)]Br2: Synthesis, solvatochromism, thermal, electrochemistry, single crystal, Hirshfeld surface analysis and antibacterial activity, Arab. J. Chem. 10 (2017) 845, https://doi.org/10.1016/j.arabjc.2016.10.008.
[26] I. Warad, A.A. Khan, M. Azam, S.I. Al-Resayes, S.F. Haddad, Design and structural studies of diimine/CdX2 (X= cl, I) complexes based on 2, 2-dimethyl-1, 3-diaminopropane ligand, J. Mol. Struct. 1062 (2014) 167, https://doi.org/10.1016/j.molstruc.2014.01.001.
[27] M. Azam, Z. Hussain, I. Warad, S. Al-Resayes, S.M. Khan, M. Shakir, A. Trzesowska-Kruszynska, R. Kruszynski, Novel Pd(ii)-salen complexes showing high in vitro anti-proliferative effects against human hepatoma cancer by modulating specific regulatory genes, Dalton Trans. 41 (2012) 10854, https://doi.org/10.1039/c2dt31143g.
[28] G.M. Morris, R. Huey, W. Lindstrom, M.F. Sanner, R.K. Belew, D.S. Goodsell, A. J. Olson, AutoDock4 and AutoDockTools4: automated docking with selective receptor flexibility, J. Comput. Chem. 30 (2009) 2785, https://doi.org/10.1002/jcc.21256.
[29] https://www.rcsb.org/structure/1BNA.
[30] H.M. Berman, J. Westbrook, Z. Feng, G. Gilliland, T.N. Bhat, H. Weissig, I. N. Shindyalov, P.E. Bourne, Nucleic Acids Res. 28 (2000) 235.
[31] T. Chen, X. Shu, H. Zhou, F.A. Beckford, M. Misir, Algorithm selection for protein–ligand docking: strategies and analysis on ACE, Sci. Rep. 13 (2013) 1–15, https://doi.org/10.1038/s41598-023-35132-5.
[32] A. Sharma, N. Dhingra, H.L. Singh, S. Khaturia, U. Bhardawaj, New complexes of organotin(IV) and organosilicon(IV) with 2-{(3,4-dimethoxybenzylidene)amino}-benzenethiol: synthesis, spectral, theoretical, antibacterial, docking studies, J. Mol. Struct. 1261 (2022) 132812, https://doi.org/10.1016/j.molstruc.2022.132812.
[33] N. Dhingra, J.B. Singh, H.L. Singh, Synthesis, spectroscopy, and density functional theory of organotin and organosilicon complexes of bioactive ligands containing nitrogen, sulfur donor atoms as antimicrobial agents: in vitro and in silico studies, Dalton Trans. 51 (2022) 8821–8831, https://doi.org/10.1039/d2dt01051h.
[34] BIOVIA and Dassault Syste'Mes, Discovery Studio Visualizer 19, Dassault Syste'Mes, San Diego, 2020.
[35] P.A. Wayne, Performance standards for antimicrobial susceptibility tests, Approved standards, NCCLS, PA, USA, 1999.
[36] P.A. Wayne, National Committee for Clinical Laboratory Standards Methods for Dilution antimicrobial susceptibility tests for bacteria that grow aerobically: approved standards- fifth edition. NCCLS document M7-A5, NCCLS, PA, USA, 2000.
[37] Ş.D. Doğan, E. Özcan, Y. Çetinkaya, M.İ. Han, O. Şahin, S.S. Bogojevic, J. Nikodinovic-Runic, M.G. Gündüz, Linking quinoline ring to 5-nitrofuran moiety via sulfonyl hydrazone bridge: synthesis, structural characterization, DFT studies, and evaluation of antibacterial and antifungal activity, J. Mol. Struct. 1292 (2023) 136155, https://doi.org/10.1016/j.molstruc.2023.136155.
[38] E. Ergan, R. Çakmak, E. Başaran, S.N. Mali, S. Akkoc, S. Annadurai, Molecular hybrid design, synthesis, in vitro cytotoxicity, in silico ADME and molecular docking studies of new benzoate ester-linked arylsulfonyl hydrazones, Molecules 29 (2024) 3478, https://doi.org/10.3390/molecules29153478.
[39] K.N.C. Prathap, N.K. Lokanath, Three novel coumarin-benzenesulfonylhydrazide hybrids: synthesis, characterization, crystal structure, Hirshfeld surface, DFT and NBO studies, J. Mol. Struct. 1171 (2018) 564, https://doi.org/10.1016/j.molstruc.2018.06.022.
[40] M.R. Aouad, M. Messali, N. Rezki, N. Al-Zaqri, I. Warad, Single proton intramigration in novel 4-phenyl-3-((4-phenyl-1H-1,2,3-triazol-1-yl)methyl)-1H-1,2,4-triazole-5(4H)-thione: XRD-crystal interactions, physicochemical, thermal, Hirshfeld surface, DFT realization of thiol/thione tautomerism, J. Mol. Liq. 264 (2018) 621, https://doi.org/10.1016/j.molliq.2018.05.085.
[41] M. Sunjuk, L. Al-Najjar, M. Shtaiwi, B. El-Eswed, K. Sweidan, P. Bernhardt, H. Zalloum, L. Al-Essa, Metal complexes of Schiff bases prepared from quinoline-3-carbohydrazide with 2-nitrobenzaldehyde, 2-chlorobenzaldehyde and 2,4-dihydroxybenzaldehyde: structure and biological activity, Inorganics 11 (2023) 412, https://doi.org/10.3390/inorganics11100412.
[42] J. Tauc, R. Grigorovici, A. Vancu, Optical properties and electronic structure of amorphous germanium, Phys. Status Sol. B 152 (1966) 627, https://doi.org/10.1002/pssb.19660150224.
[43] J. Costa, R. Taveira, C. Lima, A. Mendes, L. Santos, Optical band gaps of organic semiconductor materials, Opt. Mater. 58 (2016) 51, https://doi.org/10.1016/j.optmat.2016.03.041.
[44] A. Kösea, Ö. Güngör, J.N. Ballı, S. Erkan, Synthesis, characterization, non-linear optical and DNA binding properties of a Schiff base ligand and its cu(II) and Zn(II) complexes, J. Mol. Struct. 1268 (2022) 133750, https://doi.org/10.1016/j.molstruc.2022.133750.
[45] C.A. Lipinski, Lead-and drug-like compounds: the rule-of-five revolution, Drug Discov. Today Technol. 4 (2004) 337, https://doi.org/10.1016/j.ddtec.2004.11.007.
[46] D.E. Clark, S.D. Pickett, Computational methods for the prediction of 'drug-likeness', Drug Discov. Today 5 (2000) 49, https://doi.org/10.1016/s1359-6446(99)01451-8.
[47] Y.M.A. Aziz, M.S. Nafie, P.A. Hanna, S. Ramadan, A. Barakat, M. Elewa, Synthesis, docking, and DFT studies on novel Schiff Base sulfonamide analogues as selective COX-1 inhibitors with anti-platelet aggregation activity, Pharmaceuticals 17 (2024) 710, https://doi.org/10.3390/ph17060710.
[48] D.F. Veber, S.R. Johnson, H.-Y. Cheng, B.R. Smith, K.W. Ward, K.D. Kopple, Molecular properties that influence the oral bioavailability of drug candidates, J. Med. Chem. 45 (2002) 2615–2623, https://doi.org/10.1021/jm020017n.
[49] A. AlAli, M. Al-Noaimi, A. AlObaid, H.A. Khamees, A. Zarrouk, K. Kumara, I. Warad, S.A. Khanum, Jahn-Teller distortion in SP-like [Cu(bipy)(triamine)].2BF4 complexes with novel NH… F/CH…F synthon: XRD/HSA-interactions, physicochemical, electrochemical, DFT, docking and COX/LOX inhibition, J. Mol. Liq. 387 (2023) 122689, https://doi.org/10.1016/j.molliq.2023.122689.
[50] A. Hamad, M.A. Khan, K.M. Rahman, I. Ahmad, Z. Ul-Haq, S. Khan, Z. Shafiq, Development of sulfonamide-based Schiff bases targeting urease inhibition: synthesis, characterization, inhibitory activity assessment, molecular docking and ADME studies, Bioorg. Chem. 102 (2020) 104057, https://doi.org/10.1016/j.bioorg.2020.104057.
[51] M. Çınarlı, Ç.Y. Ataol, C.T. Zeyrek, H. Öğütcü, L. Açık, H. Batı, Design, synthesis, characterization, theoretical calculations, molecular docking studies, and biological evaluation of new Fe(II) and cu(II) complexes of 2-acetylpyridine derivative sulfonyl hydrazone Schiff Base, J. Mol. Struct. 1321 (2024) 140112, https://doi.org/10.1016/j.molstruc.2024.140112.
[52] H.L. Singh, S. Varshney, A.K. Varshney, Synthesis and spectroscopic studies of organotin(IV) complexes of biologically active Schiff bases derived from sulpha drugs, Appl. Organomet. Chem. 14 (2000) 212–217, https://doi.org/10.1002/(SICI)1099-0739(200004)14:4<212::AID-AOC980>3.0.CO;2-H.
[53] A.K. Varshney, S. Varshney, M. Sharma, H.L. Singh, SYNTHETIC, SPECTRAL AND BIOLOGICAL STUDIES OF ORGANOSILICON (IV) COMPLEXES WITH SCHIFF BASES OF SULFA DRUGS, Phosphorus Sulfur Silicon Relat. Elem. 161 (2000) 163–172, https://doi.org/10.1080/10426500008042104.